Environ. Sci. Technol. **1998**, *32,* 3155−3161

Kinetics of the Laser-Induced Photoreduction of U(VI) in Aqueous Suspensions of TiO_2 Particles

VÉRONIQUE ELIET AND GIOVANNI BIDOGLIO*

Environment Institute, Joint Research Center, European Commission, 21020 Ispra (VA), Italy

The reduction of U(VI) to U(IV) in aqueous suspensions of TiO_2 (pH 4.5−7) was investigated by time-resolved laser-induced fluorescence (TRLIF). The laser irradiation was used both to provide the energy necessary for the photogeneration of charge carriers and to monitor the kinetics of the oxidation state change directly in the measurement cuvette by exciting the U(VI) fluorescence. The U(VI) photoreduction was found to involve only adsorbed uranium species. The TRLIF measurements of U(VI) fluorescence lifetimes and individual emission fluorescence spectra allowed a selective identification of the various U(VI) hydro complexes present in the aqueous phase and adsorbed on the mineral surface. A reaction mechanism is proposed based on the kinetics results obtained at pH 7 where adsorption of the hydroxocomplex $(UO_2)_3(OH)_5^-$ on TiO_2 is complete.

Introduction

Thermodynamics predicts U(VI) as the most stable oxidation state of uranium in oxygenated surface waters, where it forms soluble complexes with hydroxide and carbonate ions and natural organic substances (*1*−*3*). The reduction to tetravalent uranium, thermodynamically unstable in an oxygenated environment, requires therefore an energy source. As U(VI) absorbs light in the wavelength range of the solar spectrum, the energy needed to produce these oxidation state changes might be supplied by solar radiation. Although uranyl ions are known to be easily photoreduced in an acid medium, this is not so easy to take place in neutral aqueous solutions because structural changes imposed by hydrolysis reactions protect U(VI) against photoreduction (*4*). However, the situation may be different at mineral−water interfaces. Several studies have shown that the redox behavior of certain species in the adsorbed state is different from that in homogeneous solution (*5*). With this respect, minerals exihibiting semiconducting properties (e.g., sulfur-containing minerals and zinc, iron, or titanium oxides) are particularly interesting.

The objective of this paper was to investigate the kinetic mechanism of the possible photochemical generation of U(IV) in a heterogeneous oxygenated medium, using titanium dioxide as a model of particles with semiconducting properties (*6*). The experiments were performed by time-resolved laser-induced fluorescence. A laser beam of appropriate wavelength provided energy both for U(VI) reduction through the photogeneration of charge carriers (h^+, e^-) at the TiO_2−water interface and for the excitation of the fluorescence of adsorbed U(VI) species. The time resolution of the fluorescence signal allowed us to measure small U(VI) concentrations in a noninvasive way even in the heterogeneous medium. Thus, it was possible to follow the kinetics of the U(VI) photoreduction directly in the measurement cuvette, since reduced U(IV) species in a noncomplexing aqueous medium do not exhibit any fluorescence property.

* Corresponding author e-mail: giovanni.bidoglio@jrc.it; fax: +39-332.78.93.28; telephone: +39.332.78.93.83.

Experimental Section

Preparation of Suspensions. A stock solution of uranyl perchlorate was prepared by dissolving uranyl nitrate in concentrated perchloric acid and heating until total evaporation of HNO_3. The remaining solid was dissolved in doubly distilled water (Millipore). A 100 ppm suspension of titanium dioxide (Degussa P25, anatase 80%, 55 m^2/g) in water was equilibrated for one night by bubbling a N_2/O_2 mixture in proportions corresponding to their atmospheric composition (80/20%). This assured the removal of all dissolved CO_2. The U(VI)−TiO_2 samples were then prepared by appropriate dilution of the two stock solutions. To prevent further risks of contamination by atmospheric CO_2, the sample preparation was always carried out in a glovebag under a N_2/O_2 atmosphere. The acidity of the U(VI)−TiO_2 suspensions was adjusted by using dilute solutions of perchloric acid and carbonate-free sodium hydroxide. A glass electrode (Radiometer, model GK2421C) filled with a saturated solution of 3 M KCl and a Radiometer pH-meter (model PHM 84) were used for pH measurements of the suspensions. After pH adjustment, the suspensions were put into Sovirel glass tubes and shaken for 3 days in the dark under N_2/O_2 atmosphere [analyses of U(VI) in the supernatant (*7*) showed that the attainment of equilibrium required about 3 h at pH 7; see Supporting Information]. Two-milliliter aliquots of these U(VI)−TiO_2 suspensions were then put into a closed quarz cuvette of 1 cm optical path and immediately subjected to laser irradiation and fluorescence measurement. Small magnetic stirrers (Hellma) directly placed into the cuvette were used to keep the TiO_2 powder in suspension, thus allowing a larger particle surface to be irradiated by the laser beam. The pH of the suspension was measured at the end of the photochemical experiments directly in the cuvette, also under a N_2/O_2 atmosphere. All fluorescence measurements were performed at a constant temperature of 21.5 °C (± 0.5) using a thermostated cuvette holder (Haake, model F3).

Laser Irradiation and Time-Resolved Fluorescence Measurements. The TiO_2 semiconductor has a band gap of about 3.1 eV, which corresponds to a wavelength of 390 nm. Thus, irradiation with a wavelength lower than 390 nm provides the TiO_2 particles with the energy necessary to cross the band gap and create very reactive charge carriers.

The irradiation was carried out with a Nd:YAG laser (Continuum, model Surelite) pumping a dye laser set to 308 nm. Under these conditions, we were able not only to excite the U(VI) and observe its fluorescence emission but also at the same time to provoke the U(VI) reduction thanks to the electrons of the conduction band. The formation of nonfluorescent U(IV) resulted in an immediate decrease of the fluorescence signal of amplitude depending on the irradiation intensity. The fluorescence was measured until steady state was obtained or until the U(VI) fluorescence disappeared completely. The measurement time thus varied between 4 and 15 min. The U(VI) fluorescence was collected at a right angle to the excitation beam and focused onto the entrance slit of a monochromator set at 512 nm (Jobin-Yvon, model THR 1000). A gated photomultiplier tube (Hamamatsu,

S0013-936X(97)00929-2 CCC: $15.00
Published on Web 09/12/1998

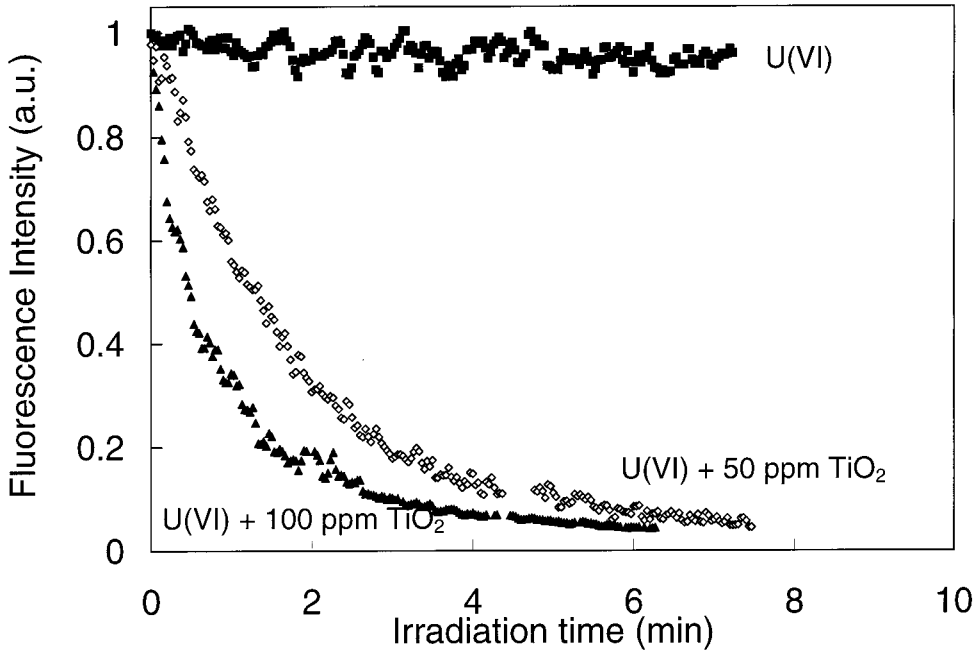

FIGURE 1. Influence of different concentrations of TiO_2 on the fluorescence signal of U(VI). The fluorescence intensity is given in arbitrary units (a.u.). pH 6.5, $C_{U(VI),T} = 10^{-5}$ M, $\lambda_{exc} = 308$ nm, $\lambda_{emi} = 512$ nm.

model R1333) opening at 1 μs after the laser pulse was used to reject the scattering of the laser light on the semiconductor particles and detect the fluorescence of U(VI) (for further details see Supporting Information).

The lifetimes and the emission spectra of the fluorescent uranium species in the TiO_2 suspensions were measured before and after each photochemical experiments by using a very low laser intensity to avoid U(VI) photodegradation. For all suspensions at pH > 5, the U(VI) fluorescence lifetimes were determined between 1 and 101 μs with a measurement window of 60 μs. The fluorescence decay curves thus obtained were analyzed by a statistical procedure using the nonlinear regression program NLIN of the SAS/STAT software package (*6, 8*).

Ferrioxalate actinometry (*9*) with $[K_3Fe(C_2O_4)_3] = 2.4 \times 10^{-3}$ M was used to calibrate the light flux into the cell. However, the light flux actually absorbed by the TiO_2 was less than that measured, due to reflection on the cuvette walls and light scattering on the suspended particles.

Results and Discussion

In the investigated pH range (4−7), no photoreduction of U(VI) was observed in homogeneous solutions irradiated at 308 nm (Figure 1). However, a net decrease with time of the U(VI) fluorescence signal was found when irradiating TiO_2-containing suspensions, with a pH dependence very similar to that of U(VI) adsorption on the mineral oxide. No U(VI) reduction occurred at acidic pH where adsorption was rather low (about 10% at pH 4.5), whereas photoreduction was observed to increase with pH [U(VI) adsorption at pH 5 and pH 7 was respectively 50% and 100%]. Figure 2 shows the kinetic curves obtained on irradiating 50 ppm TiO_2 suspensions at pH 6.5 containing different total concentrations of U(VI). The photoreduction appears to be faster at lower U(VI) concentrations because of the relatively greater amount of adsorbed uranium.

To confirm the photocatalytic role of TiO_2 in the photoreduction of U(VI), a TiO_2 suspension at pH 7 was irradiated at 433 nm, which corresponds to a peak of the U(VI) excitation spectrum (*8*). In this case, the energy supplied to the semiconductor is lower than the band gap barrier, and the photochemical reaction is not expected to occur because no electrons can be promoted to the conduction band. Accordingly, the fluorescence signal of U(VI) in the suspension was observed to remain constant even for very long irradiation times. Additional experiments involved irradiation of U(VI) at 308 nm in suspensions of mineral oxide with no photocatalytic properties, i.e., Al_2O_3 (50 ppm) at the same surface area as in the case of TiO_2. Under these conditions (pH 7), U(VI) adsorption was in the order of 95% on alumina. Even for very high laser intensities, no reduction of U(VI) was observed.

Fluorescence Characteristics of U(VI) Species in the Heterogeneous Medium. Figure 3 shows the aqueous speciation diagram of U(VI) as a function of pH, where (m,n) denotes the various $(UO_2)_m(OH)_n^{2m-n}$ species. However, the speciation is likely to be different in the heterogeneous medium because of uranium adsorption on TiO_2. Attempts were made to determine the number and nature of the U(VI) chemical species in the suspensions on the basis of their fluorescence lifetimes. Their knowledge would help to elaborate a mechanism accounting for the photochemical reaction.

Table 1 reports the fluorescence lifetimes of the U(VI) hydroxo species at the temperature of the present experiments (21.5 °C), derived from previously published data at 25 °C (*8*) using the activation energies reported in refs *6* and *10*. These values can be compared with those measured in the present work when TiO_2 was added to the solutions. The experimental results at different pH are reported in Table 2. Two distinct lifetimes could be detected at pH 4.6, both in the presence and in the absence of TiO_2. The speciation diagram (Figure 3) shows that the uranyl ion and the (1,1) and (2,2) complexes are present in the solution. According to Table 1, the longest lifetime is associated to the species (1,1), whereas the shortest one appears to be the uranyl ion. The species (2,2) is present in too small quantities to be identified during the statistical deconvolution of the fluorescence decay curves. The same lifetimes and the same spectra were obtained for the solutions both with and without TiO_2 (Figure 4). This is not surprising because adsorption experiments as a function of pH showed that most of the U(VI) is present as aqueous species at pH 4.6 (see Supporting Information).

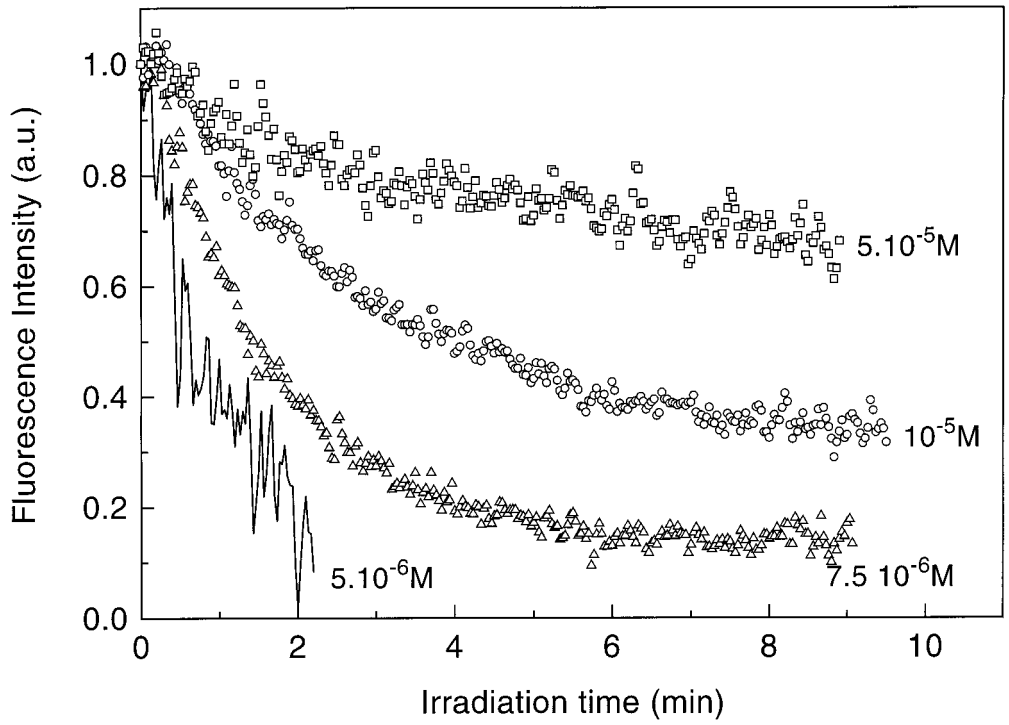

FIGURE 2. Fluorescence signals of different total concentrations of U(VI) in 50 ppm suspensions of TiO_2. pH 6.5, $\lambda_{exc} = 308$ nm, $\lambda_{emi} = 512$ nm.

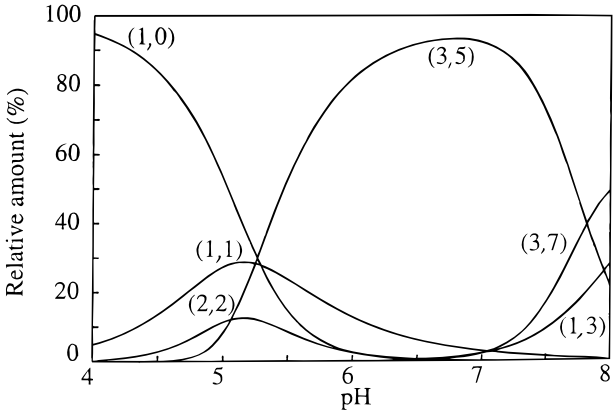

FIGURE 3. Speciation diagram of U(VI) as a function of pH. (*m,n*) refers to the hydroxo complex $(UO_2)_m(OH)_n^{2m-n}$. The equilibria used for the calculations and the corresponding stability constants are reported in a previous paper *(8)*. The solid lines represent average values. $C_{U(VI),T} = 10^{-5}$ M, $I = 0$, $T = 21.5$ °C.

TABLE 1. Fluorescence Lifetimes of U(VI) Species at $T = 21.5$ °C

species	lifetime (μs)
UO_2^{2+}	2.2 ± 0.1
UO_2OH^+	40.5 ± 8.9
$(UO_2)_2(OH)_2^{2+}$	13 ± 4.5
$(UO_2)_3(OH)_5^-$	24.3 ± 1.8

A spectral change was observed when the pH was increased to 5.4 (Figure 4). The statistical analysis identified only one fluorescent component with an identical lifetime, in the uncertainty range considered, both for the solution and the suspension. Table 1 suggests that this corresponds to the lifetime of the aqueous species (3,5), predominant at this pH (Figure 3).

With a further increase of pH to 6.1, the (3,5) complex remains the predominant aqueous species (Figure 3).

TABLE 2. pH Dependence of Fluorescence Lifetimes of Uranium Species in TiO_2 Suspensions and Aqueous Solutions with no TiO_2[a]

pH	contact time	lifetime 1 (μs)	lifetime 2 (μs)
4.6[b]	3 day	2.55 ± 0.6	35.8 ± 5.2
4.6[c]	3 day	3.7 ± 0.8	42 ± 9
5.4[b]	3 day	*d*	23.1 ± 1.2
5.45[c]	3 day	*d*	23.1 ± 0.5
5.9[b]	3 day	*d*	26.6 ± 1.1
6.1[b]	3 h	*d*	28.3 ± 1.0
7.1[b]	3 h	*d*	30.0 ± 1.1
7.1[b]	3 day	*d*	30 ± 0.6
7.2[c]	3 h	*d*	24.0 ± 0.8

[a] The reported values are the average of different experimental results. The uncertainty is twice the standard deviation. $C_{U(VI)} = 10^{-5}$ M, T = 21.5 °C, $\lambda_{exc} = 308$ nm, $\lambda_{emi} = 512$ nm, gate width = 60 μs, delay = 1 μs. [b] 100 ppm TiO_2 suspension. [c] Aqueous solution with no TiO_2. [d] nondetected.

However, a lifetime slightly higher than at pH 5.4 was measured. The adsorption experiments of U(VI) on TiO_2 showed that more than 80% of the uranium is adsorbed at pH 6, while about 60% of the U(VI) is adsorbed at pH 5.5. It is then possible that the difference in lifetime is due to a greater contribution of the (3,5) species adsorbed on the TiO_2 at pH 6.1. This hypothesis is confirmed by the suspensions at pH 7.1 where adsorption is complete and for which only one species is detected, with an average fluorescence lifetime of 30 ± 0.6 μs. This is higher than the lifetime measured for the polynuclear species (3,5) in homogeneous aqueous solution (Table 1) and suggests a surface complexation process of the (3,5) species on TiO_2. Also the fluorescence spectrum of the adsorbed (3,5) species differs slightly from that recorded in the absence of TiO_2 (Figure 4).

Photoreduction at Different Light Intensities and pH. Figure 5a,b shows the kinetic curves of U(VI) disappearance in 100 ppm suspensions of TiO_2. For comparison, these curves are all referred to the initial fluorescence value of the

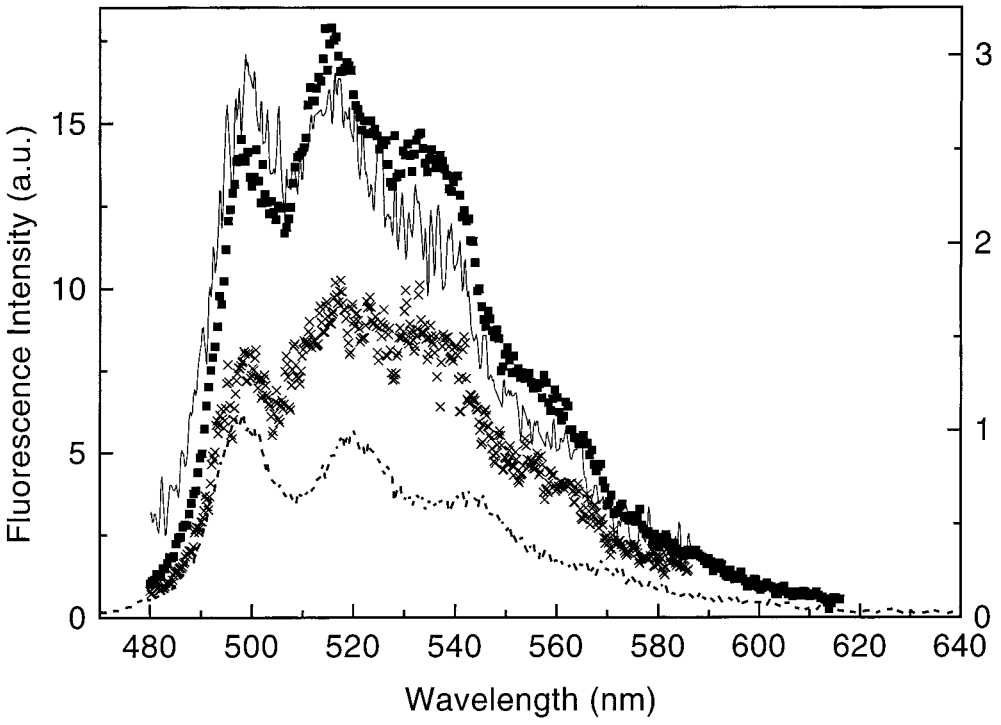

FIGURE 4. Time-resolved fluorescence emission spectra of 10^{-5} M U(VI) in aqueous solution (left-hand ordinate) at pH 4.6 (dashed line), pH 5.1 (cross line), and pH 7.1 (solid line) and in the presence of 100 ppm TiO_2 after 3 days of contact time at pH 7.1 (squared line, right-hand ordinate). $\lambda_{exc} = 308$ nm.

suspension at time zero. Whatever the suspension pH, the U(VI) fluorescence signal decreases more rapidly as the irradiation intensity becomes higher. This phenomenon is even more important when increasing the TiO_2 concentration. One can also observe that all the curves reach a steady state after a certain time, which depends not only on the incident laser intensity but also on the pH. At high laser intensity and at high pH, where the U(VI) adsorption is considerable, one can observe that the U(VI) to U(IV) reduction is complete, while at pH 5.1, where adsorption is weak, the attainment of steady state takes place earlier.

A systematic reduction of the pH after irradiation (about 0.3 pH unit) was measured only for the suspensions at pH 7. A pH decrease has been reported to occur also for other metals, such as Hg, Au, and Pb, in the presence of TiO_2 (*11*−*13*). However, the pH variation in the present experimental conditions only sligthly affected the extent of U(VI) adsorption (>90%).

Mechanism of U(VI) Photoredox Reactions. The conditions at pH 7 when all uranium is adsorbed are considered here to investigate the U(VI) photoreduction mechanism. Under these conditions, the measured U(VI) fluorescence is directly related to the concentration of the adsorbed species, i.e.

$$F_{tot} = F_{ads} = K(\eta\epsilon)_{ads}\mathrm{SF}[3,5]_{ads} \exp\left(-\frac{t_{F1}}{\tau_{ads}}\right) \qquad (1)$$

where K is a constant depending on experimental conditions (intensity of laser beam, position of the cuvette, etc), the product $(\eta\epsilon)$ is the fluorescence efficiency of the (3,5) species adsorbed (*8*), SF is a screening factor that takes into account the light scattering due to the particles in the suspension, [3,5] is the concentration of (3,5) adsorbed, τ_{ads} is its fluorescent lifetime, and t_{F1} is the delay imposed by the time gating of the detection system. Since during a typical experiment all these parameters are constant with the exception of the concentration of the adsorbed (3,5) species that undergoes photoreduction, it is possible to write

$$F_{total} = F_{ads} = \gamma[3,5]_{ads} \qquad (2)$$

where γ is an overall proportionality factor that can be determined at time 0 of the kinetic curve, when the adsorbed concentration is equal to the total concentration U_T. One can thus calculate, for each point t of the kinetic curve, the concentration of U(VI) on behalf of the following equation:

$$([3,5]_{ads})_t = \frac{U_T}{(F)_{t_0}}(F)_t \qquad (3)$$

To establish a kinetic photoreduction model for U(VI) in the presence of TiO_2, all reactions taking place in the system have to be considered: the photogeneration of charge carriers, the reduction of the uranium species at the semiconductor surface, and their competitive reoxidation (Table 3, containing eqs 4−18). Available information does not permit a detailed mechanistic analysis in terms of elementary reactions representing molecular level events. Moreover, the lack of literature studies on uranium photochemistry in noncomplexing neutral pH media is certainly not helpful. Empirical rate equations showing how overall rates depend on reactant and product concentrations are therefore proposed, with uranium species simply represented by their oxidation state number.

U(VI) Photoreduction Mechanism at the TiO_2 Surface. Although the only uranium species present at pH 7 is the hydrolyzed complex (3,5) (Figure 3), it is unlikely that its photoreduction takes place through a multielectron process, generally slower and consequently less probable than that involving a smaller number of electrons:

$$(UO_2)_3(OH)_5^+ + 5H^+ + 3e_{cb}^- \rightarrow 3UO_2^+ + 5H_2O \quad (19)$$

Therefore, eq 19 may be reasonably broken down into three steps: each corresponding to the transfer of one electron, with the first step likely to be the rate determining

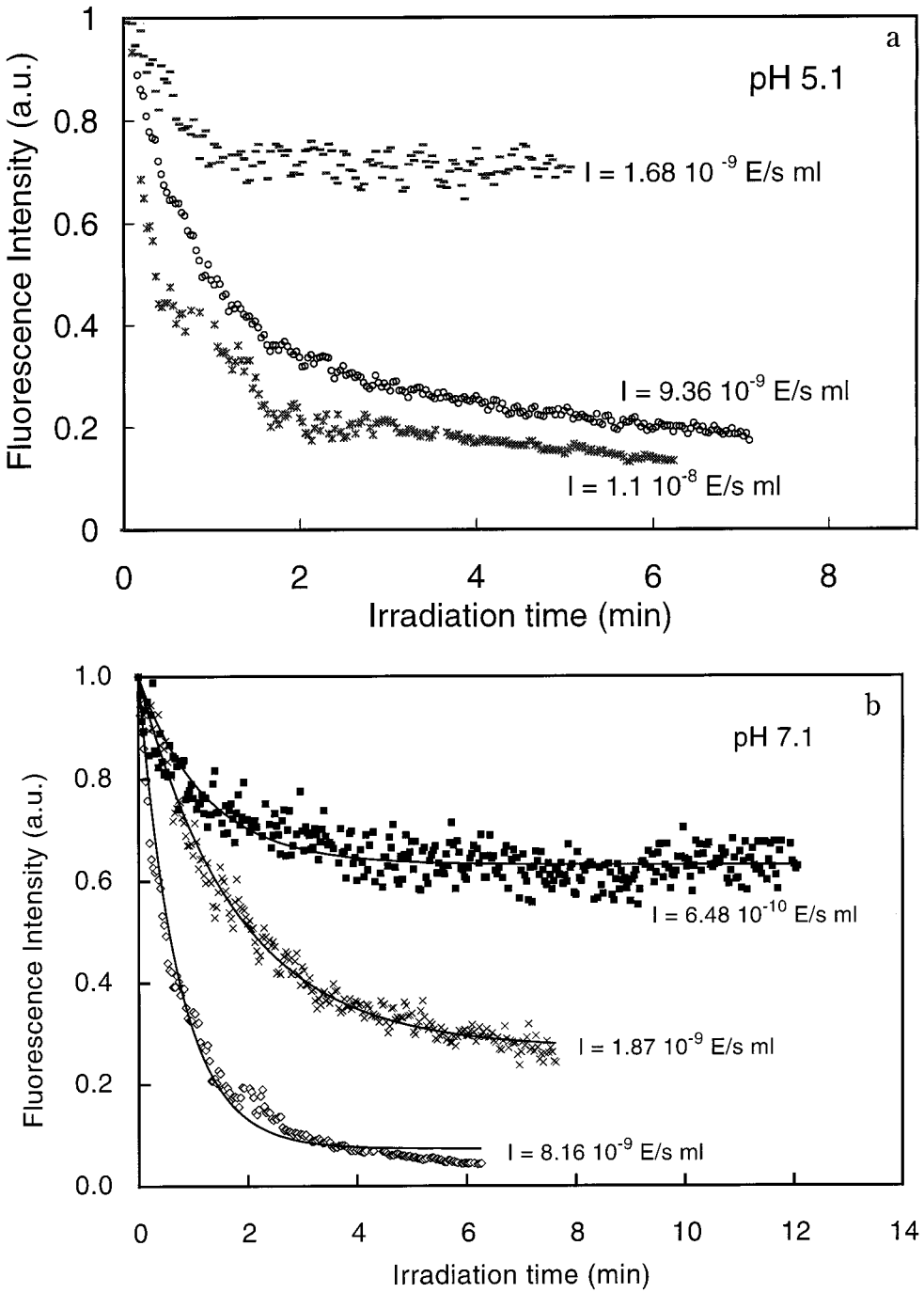

FIGURE 5. Kinetics of U(VI) photoreduction in 100 ppm TiO_2 suspensions at different pH (5.1, panel a; 7.1, panel b) and for different irradiation intensities (units: Einstein s^{-1} mL^{-1}). $C_{U(VI),T} = 10^{-5}$ M, $\lambda_{exc} = 308$ nm, $\lambda_{emi} = 512$ nm. The solid lines in panel b represent the fit of the experimental data according to the model eq 24.

one because of the structural change involved in the reduction of the (3,5) species (eq 12 in Table 3).

The rate constant for the reduction of Np(V), a chemical analogue of U(V), with water radiolysis products, i.e., e^-_{aq}, H_2O_2, $OH^\bullet$, $H^\bullet$, $HO_2^\bullet$, similar to those produced at the TiO_2 surface, has been found to be close to the rate of a reaction controlled by the diffusion of molecules in solutions (*23*−*26*). Taking also into account the thermodynamic instability of U(V) in the neutral pH range, UO_2^+ ions once formed would not have time to migrate into the solutions (even though they exhibit very little tendency for adsorption) because they are immediately reduced to U(IV) (eq 13, Table 3). This oxidation state of uranium, existing as the hydroxo complex $[U(OH)_4]_{aq}$ in the pH range studied (*3*), tends to equilibrate with a solid amorphous hydroxide:

$$[U(OH)_4]_{aq} \leftrightharpoons UO_2 \cdot 2H_2O_{(am)} \qquad (20)$$

slowly transforming with time in a crystalline form of much lower solubility. For the amorphous form, Bruno et al. (*27*) determined a solubility product of $\log K_s = -4.4 \pm 0.2$ in 0.5 M $NaClO_4$. This would correspond to a solubility limit higher than the 10^{-5} M concentration used in the present work. This value, however, has been questioned by Rai et al. (*28*), who determined a $\log K_s$ several orders of magnitude lower. The actual form under which U(IV) is present in our conditions depends then on the precipitation kinetics of the amorphous compound. Since this has been reported to be

TABLE 3. Reactions Used in the Formulation of the Mechanism for the Photoreduction of Uranium Species Adsorbed on TiO_2 Particles

	eq	ref
Charge Carrier Generation		
$TiO_2 \xrightarrow{\phi I_A} e^-_{cb} + h^+_{vb}$	4	*14*
$e^-_{cb} + h^+_{vb} \xrightarrow{k_5} TiO_2 + \text{heat (or } h\nu)$	5	*14*
$OH^-_{sup} + h^+_{vb} \xrightarrow{k_6} OH^\bullet$	6	*12*, *15*−*17*
$2OH^\bullet \xrightarrow{k_7} H_2O_2$	7	*18*−*20*
$2H_2O + 2h^+_{vb} \xrightarrow{k_8} H_2O_2 + 2H^+$	8	*18*, *21*
$O_2 + 2e^-_{cb} + 2H^+ \xrightarrow{k_9} H_2O_2$	9	*18*, *21*
$H_2O_2 + 2h^+_{vb} \xrightarrow{k_{10}} O_2 + 2H^+$	10	*17*, *22*
$H_2O_2 + 2e^-_{cb} + 2H^+ \xrightarrow{k_{11}} 2H_2O$	11	*17*, *22*
Reduction of Uranium Species Adsorbed on TiO_2 Particles		
$[U(VI)] + e^-_{cb} \xrightarrow{k_{12}} [U(V)]$	12	
$[U(V)] + e^-_{cb} \xrightarrow{k_{13}} [U(IV)_{aq}]$	13	
Oxidation of Uranium Species Adsorbed on TiO_2 Particles		
$[U(V)] + OH^\bullet \xrightarrow{k_{14}} [U(VI)]$	14	
$[U(IV)_{aq}] + OH^\bullet \xrightarrow{k_{15}} [U(V)] + OH^-$	15	
$[U(IV)_{aq}] + O_2 \xrightarrow{k_{16}} [U(V)]$	16	
$[U(V)] + O_2 \xrightarrow{k_{17}} [U(VI)]$	17	
$[U(IV)_{aq}] \leftrightarrow [U(IV)_{am}] + O_2 \rightarrow U(IV-VI)_s \xrightarrow{\text{slow}} U(VI)_s$	18	

rather slow (*29*), during the irradiation experiments (generally, not longer than 10 min), the U(IV) formed is likely to remain as a neutral aqueous species.

Photooxidation of U(IV) and U(V). Competitive oxidation of reduced uranium species may occur, involving both $OH^\bullet$ radicals, major oxidants at TiO_2 surface (*12*, *15*−*17*, *19*), and molecular oxygen (eqs 14−17 in Table 3). The rate constants for the reaction between $OH^\bullet$ radicals and inorganic reductants, in the order of 10^6−10^{10} M^{-1} s^{-1} in a homogeneous medium (*23*), are expected to be even greater at the semiconductor surface where sorbed species and photogenerated $OH^\bullet$ are directly in contact. In addition to the oxidation of U(IV) and U(V), the molecular oxygen adsorbed on the TiO_2 surface can form the oxidizing ion O_2^- by capturing conduction band electrons (*13*, *21*, *30*). Oxidation by hydrogen peroxide has not been taken into account in Table 3 because the H_2O_2 formed is very rapidly assimilated in the TiO_2 structure and photodegraded (*22*).

At sufficiently high irradiation intensities, the fluorescence signal disappeared in a few minutes. After standing 2 h in the dark, a small fluorescence signal that did not evolve anymore with time could be measured again. It appears that uranium reoxidation did not lead to the starting hydroxo complex of U(VI). Amadelli et al. (*31*) recorded the infrared spectra of the uranium species adsorbed on TiO_2 after irradiation at 360 nm. They found a compound with a structure similar to that of U_3O_8 [mixed U(VI)−U(IV) oxide], reoxidizing in air and remaining on TiO_2 as UO_3. Similarly, Adams et al. (*32*) and Dodge et al. (*33*) reported the formation of an insoluble uranium species (an hydrated UO_3 oxide) after several days of irradiation of U(VI)−citrate solutions. Moreover, Christensen et al. (*34*) developed a kinetic model of the oxidation mechanism of UO_2 by water radiolysis products, leading eventually to the formation of the oxide $UO_3 \cdot 2H_2O$.

On this basis, it seems that the formation of an oxide is another reaction that must be taken into account to describe the mechanism correctly (eq 18, Table 3). However, the reported oxidation kinetics to form UO_3 are much longer (several days) than the duration of our experiments. Therefore, complete oxidation could not occur. The stable nonfluorescent end product of the photoreduction was likely to be an oxide of structure intermediate between UO_2 and UO_3, possibly the U_3O_8 suggested by Amadelli et al. (*31*).

Kinetic Model. With reference to Table 3, the time dependence of the concentration of the adsorbed U(VI) species can be written as

$$\frac{d[U(VI)]_{ads}}{dt} = -k_{12}[e^-_{cb}][U(VI)]_{ads} + (k_{14}[OH^\bullet] + k_{17}[O_2])[U(V)] \quad (21)$$

On the basis of the steady-state assumption for the intermediate U(VI) ions, the species e^-_{cb}, h^+_{vb} and $OH^\bullet$ and making the hypotheses that (i) oxidation of the U(V) and U(IV) species is faster with $OH^\bullet$ radicals than with adsorbed molecular oxygen and (ii) the quantity of U(IV) formed is the same as the quantity of U(VI) disappeared; it can be shown (see Supporting Information) that eq 21 reduces to

$$\frac{d[U(VI)]_{ads}}{dt} = -A[U(VI)]_{ads} + B \quad (22)$$

where A and B depend on the total concentration of uranium, U_T, the irradiation intensity, I_A, and the quantum yield, ϕ, of the excitation process.

The mathematical resolution of this differential equation is

$$[U(VI)]_{ads} = C_1 \exp^{-At} + \frac{B}{A} \quad (23)$$

where C_1 is an integration constant that can be determined for $t = 0$, when the concentration of the adsorbed U(VI) species is equal to the total concentration U_T, yielding:

$$[U(VI)]_{ads} = U_T \exp^{-At} + \frac{B}{A}(1 - \exp^{-At}) \quad (24)$$

where

$$A = \frac{\left(k_{12}k_{13}\frac{\phi I_A}{k_5} + k_{14}k_{15}\frac{k'_6}{k_7}\left(\frac{\phi I_A}{k_5}\right)^{1/2}\right)}{k_{13}\left(\frac{\phi I_A}{k_5}\right)^{1/2} + k_{14}\left(\frac{k'_6}{k_7}\right)^{1/2}\left(\frac{\phi I_A}{k_5}\right)^{1/4}} \quad (25)$$

$$\frac{B}{A} = \frac{U_T}{\frac{k_{12}k_{13}\left(\frac{\phi I_A}{k_5}\right)^{1/2}}{k_{14}k_{15}\frac{k_6[OH^-]}{k_7}} + 1} \quad (26)$$

TABLE 4. Results of the Regression Analysis of the Experimental Points (100 ppm TiO_2, pH 7) with Model eq 24[a]

incident intensity (Einstein s^{-1} mL^{-1})	*A*	*B*/*A* ($\times 10^{-5}$)
6.48×10^{-10}	0.82 ± 0.06	0.632 ± 0.004
1.63×10^{-9}	0.63 ± 0.02	0.309 ± 0.008
1.87×10^{-9}	0.555 ± 0.016	0.269 ± 0.006
8.16×10^{-9}	1.39 ± 0.04	0.073 ± 0.006
1.06×10^{-8}	1.44 ± 0.04	0.019 ± 0.006

[a] The reported uncertainties are twice the standard deviation.

Equation 24 represents the competition between the reduction of the U(VI) species and the reoxidation of its reduced species. At short irradiation times and for high light intensities, the first term predominates and the decrease of the U(VI) concentration is mainly due to the U(VI) reduction. Then the second term becomes more important and the concentration of the U(VI) species tends to an asymptotic value, representing a steady state in the competition between the two processes.

Model Verification. A check of the proposed photoreduction mechanism can be made by comparing the experimental data with the model eq 24. A fit of the data (see examples in Figure 5b) with a biexponential equation with *A* and *B*/*A* as predictor variables, yielded the values reported in Table 4. The second step of the model verification consists of determining the light intensity dependence of the best fit values. A look at the equations 25 and 26 shows that the *A* and the *B*/*A* ratio depend only on the total concentration of U(VI), the ϕI_A product, and the pH. Since the pH and the uranium concentration are the same for all the suspensions, the only variable is the intensity of the laser beam. The formulation of *A* is quite complex and it is difficult to determine its relationship with the intensity. This is much easier with the *B*/*A* ratio. When the first term of the denominator of eq 26 is larger than 1, the B/A values should be inversely proportional to the square root of the irradiation intensity. Indeed, all the B/A data of Table 4 are linearly correlated to $1/I^{1/2}$, with a regression coefficient of 0.97. This can then be considered as a confirmation of the proposed model for the photoreduction of the U(VI) on the TiO_2 surface.

The reduction of U(VI) to U(IV) is possible even in an oxygenated medium, following light absorption by TiO_2, used as model semiconducting particles. The results show that U(IV) is partially stabilized, probably through the formation of a mixed precipitate with U(VI). Similar mechanisms may also occur in the oxic−photic zone of surface waters in the presence of minerals with semiconducting properties such as iron and zinc oxides.

Supporting Information Available

Adsorption measurements, time-resolved laser fluorescence measurements, and the kinetic model (6 pages). Ordering information is given on any current masthead page.

Literature Cited

(1) *1*) Giesy, J. P.; Geiger, R. A.; Kevern, N. R.; Alberts, J. J. *J. Environ. Radioact.* **1986**, *4*, 39−64.

(2) Kim, J. I. In *Handbook of the Physics and Chemistry of the Actinides*; Freeman, A. F., Keller, C., Eds.; Elsevier Science: Amsterdam, 1986; Vol. 4, pp 413−455.

(3) Grenthe, I.; Fuger, J.; Konings, R. J. M.; Lemire, R. J.; Mueller, A. B.; Nguyen-Trung, C.; Wanner, H. *Chemical Thermodynamics of Uranium*; North-Holland, NEA-TDB, OCDE: Amsterdam, 1992.

(4) Hart, E. J.; Amber, M. *The Hydrated Electron*; Wiley-Interscience: New York, 1970.

(5) Wehrli, B.; Stumm, W. *Geochim. Cosmochim. Acta* **1989**, *53*, 69.

(6) Eliet, V. Applications des techniques de fluorescence pour l'étude de l'Uranium dans des milieux homogènes et hétérogènes: réactions d'hydrolyse et photoreduction sur le bioxyde de Titane. Ph.D. Dissertation, 1996, Paris XI Orsay University, France.

(7) Mauchien, P. CEA Report R.5300, 1985, France.

(8) Eliet, V.; Bidoglio, G.; Omenetto, N.; Parma, L.; Grenthe, I. *J. Chem. Soc., Faraday Trans.* **1995**, *91* (15), 2275−2285.

(9) Hatchard, C. G.; Parker, C. A. *Proc. R. Soc.* **1956**, *A235*, 518.

(10) Eliet, V.; Bidoglio, G.; Grenthe, I. Manuscript in preparation.

(11) Borgarello, E.; Ron, H.; Serpone, N. *Nouv. J. Chim.* **1985**, *9* (12), 743−747.

(12) Serpone, N.; Lawless, D.; Terzian, R.; Minero, C.; Pelizetti, E. In *Photochemical conversion and storage of solar energy*; Pelizetti, E., Schiavello, M., Eds.; Kluwer Academic Publishers: Amsterdam, 1991; pp 451−475.

(13) Lawless, D.; Res, A.; Borgarello, E.; Harris, R.; Serpone, N.; Minero, C.; Pelizetti, E.; Hidaka, H. *Chim. Ind.* **1990**, *72*, 139−146.

(14) Linsebigler, A. L.; Lu, G.; Yates, J. T. *Chem. Rev.* **1995**, *95* (3), 735−758.

(15) Lawless, D.; Serpone, N.; Meisel, D. *J. Phys. Chem.* **1991**, *95*, (13), 3166−3170.

(16) Al-Ekabi, H.; Serpone, N. *J. Phys. Chem.* **1988**, *92*, 5726−5731.

(17) Hoffman, A. J.; Carraway, E. R.; Hoffmann, M. R. *Environ. Sci. Technol.* **1994**, *28*, 776−785.

(18) Bahnemann, D. W.; Hoffmann, M. R.; Hong, A. P.; Kormann, C. *The chemistry of acid rain*; American Chemical Society: Washington, DC, 1987; Chapter 10, pp 120−132.

(19) Kormann, C.; Bahnemann, D. W.; Hoffmann, M. R. *Environ. Sci. Technol.* **1991**, *25*, 494−500.

(20) Peterson, M. W.; Turner, J. A.; Nozik, A. J. *J. Phys. Chem.* **1991**, *95*, 221−225.

(21) Hoffmann, M. R.; Martin, S. T.; Choi, W.; Bahnemann, D. W. *Chem. Rev.* **1995**, *95* (1), 69−96.

(22) Kormann, C.; Bahnemann, D. W.; Hoffmann, M. R. *Environ. Sci. Technol.* **1988**, *22*, 798−806.

(23) Sullivan, J. C.; Gordon, S.; Cohen, D.; Mulac, W.; Schmidt, K. H. *J. Phys. Chem.* **1976**, *80* (15), 1684−1686.

(24) Schmidt, K. H.; Gordon, S.; Thompson, R. C.; Sullivan, J. C. *J. Inorg. Nucl. Chem.* **1980**, *42*, 611−615.

(25) Nash, K.; Mulac, W.; Noon, M.; Fried, S.; Sullivan, J. C. *J. Inorg. Nucl. Chem.* **1981**, *43*, 897−899.

(26) Broszkiewicz, R. K.; Vojnovic, B.; Michael, B. D. *Radiat. Phys. Chem.* **1992**, *39* (1), 137−140.

(27) Bruno, J.; Casas, I.; Lagerman, B.; Munoz, M. In *Scientific basis for nuclear waste management X*; Bates, J. K., Seefeldt, W. B., Eds.; 1987; pp 153−160.

(28) Rai, D.; Felmy, A. R.; Ryan, J. L. *Inorg. Chem.* **1990**, *29*, 260−264.

(29) Bruno, J.; Casas, I.; Puigdomenech, I. *Geochim. Cosmochim. Acta* **1991**, *55*, 647−658.

(30) Schwitzgebel, J.; Ekerdt, J. G.; Gerischer, H.; Heller, A. *J. Phys. Chem.* **1995**, *99*, 5633−5638.

(31) Amadelli, R.; Maldotti, A.; Sostero, S.; Carassiti, V. *J. Chem. Soc., Faraday Trans.* **1991**, *87* (19), 3267−3273.

(32) Adams, A.; Smith, T. D. *J. Chem. Soc.* **1960**, 4846−4849.

(33) Dodge, C. J.; Francis, A. J. *Environ. Sci. Technol.* **1994**, *28*, 1300−1306.

(34) Christensen, H.; Sunder, S.; Shoesmith, D. W. *J. Alloys Compd.* **1994**, *213*/*214*, 93−99.

Received for review October 22, 1997. Revised manuscript received June 15, 1998. Accepted June 25, 1998.

ES970929S